CSIRO PUBLISHING

Aust. J. Chem.
https://doi.org/10.1071/CH18576

Full Paper

Cellulose-Supported Ionic Liquid Phase Catalyst-Mediated Mannich Reaction

Sharanabasappa Khanapure,[A] *Megha Jagadale,*[A] *Dolly Kale,*[A] *Shivanand Gajare,*[A] *and Gajanan Rashinkar*[A,B]

[A]Department of Chemistry, Shivaji University, Kolhapur, 416004, India.
[B]Corresponding author. Email: gsr_chem@unishivaji.ac.in

Cellulose-supported ionic liquid phase (SILP) catalyst containing a camphor sulfonate anion with a pendant ferrocenyl group was prepared and characterised with different analytical techniques such as Fourier-transform infrared, Fourier-transform Raman, and cross polarization–magic angle spinning (CP-MAS) ^{13}C NMR spectroscopy, X-ray diffraction, scanning electron microscopy, and thermogravimetric analysis. The SILP catalyst displayed excellent catalytic activity in the synthesis of β-amino carbonyl compounds by Mannich reaction. Recycling studies revealed that SILP catalyst could be reused six times without significant decrease in catalytic activity.

Manuscript received: 22 November 2018.
Manuscript accepted: 18 March 2019.
Published online: 30 April 2019.

Introduction

The concept of supported ionic liquid phase (SILP) catalysis involving immobilization of ionic liquids (ILs) over the surface of porous, high-area support material has attracted enormous attention in the field of sustainable organic synthesis.[1–6] This novel class of advanced materials help to circumvent the drawbacks associated with ILs such as high cost, toxicity, and an energy-consuming distillation step for their recyclability and reusability.[7,8] The synergistic combination of the advantageous properties of ILs with those of support material enhances the performance of SILP catalysts with retention of the properties of both the species. In addition, processes employing SILP catalysts can be performed under unusual conditions using fixed-bed reactor designs.[9,10] Moreover, SILP catalysts offer unique benefits such as facile separation by filtration and significant advances in activity as well as selectivity. These fascinating properties of SILP catalysts have stimulated researchers to design diversely functionalized SILP catalysts for various organic transformations. Recent investigations have revealed that the catalytic performance of SILP catalysts primarily depends on the nature of the support material. In view of this, a large number of diverse supports such as polymer-based materials,[11–18] porous silica gels,[19,20] carbon nanotubes,[21] active carbon cloth,[22] chitosan,[23] and magnetic nanoparticles[24] have been used in the preparation of SILP catalysts. However, despite considerable progress, there is still scope to prepare new SILP catalysts, especially employing biorenewable feedstock-derived supports.

Cellulose is the most abundant natural biopolymer obtained from renewable agro-waste.[25–27] It is composed of long linear chains of repeating units of β-D-glucose linked via 1,4-glycosidic bonds. It has an unusual structure in which every glucose monomer is linked with neighbouring units through hydrogen bonds. As a result, cellulose chains are tightly packed to form a highly ordered crystal structure, making it insoluble in water as well as in common organic solvents.[28] In addition, it is cheap, non-toxic, insensitive to air and moisture, has a high surface area and a limited carbon footprint as well as excellent biodegradability.[29–34] These versatile properties have stimulated enormous interest in the use of cellulose as a support in the synthesis of various heterogeneous catalysts.

β-Amino carbonyl compounds are privileged scaffolds that are used as intermediates in the synthesis of pharmaceuticals and bio-active natural products such as antibiotics, amino alcohols, peptides, and lactams.[35] In addition, they act as precursors to optically active amino acids[36] and as building blocks to chiral molecules.[37] Given their interesting applications, the synthesis of β-amino carbonyl compounds plays a significant role both in the drug discovery process and in organic synthesis. The classical method for the synthesis of β-amino carbonyl compounds includes the Mannich reaction of aldehydes, ketones, and amines. A large number of catalytic systems have been used to increase the efficiency of the Mannich reaction.[38–43] However, many of the reported methods suffer from drawbacks such as the use of expensive metal salts as catalysts, prolonged reaction time, moisture sensitivity of the catalysts, and low yields. Therefore, there is a need to develop an efficient protocol using a highly efficient catalyst for the synthesis of β-amino carbonyl compounds.

In continuation of our work related to green chemistry,[44,45] we report herein the preparation of cellulose SILP catalyst containing a camphor sulfonate anion with a pendant ferrocenyl group, and its application as a heterogeneous catalyst in the synthesis of β-amino carbonyl compounds via the Mannich reaction.

Results and Discussion

The preparation of cellulose SILP catalyst containing a camphor sulfonate anion with a pendant ferrocenyl group is outlined in

Scheme 1. Initially, aluminium oxide (**2**) was finely dispersed on the surface of cellulose (**1**) to obtain the Cell–Al_2O_3 composite (**3**) with high degree of adhesion following the literature procedure.[46,47] The formation of stable Al–O–Si bonds through reaction of Al–OH groups of **3** and Si–OEt groups of (3-chloropropyl) triethoxy silane (**4**) resulted in the formation of chloropropyl cellulose (**5**) with a significant degree of organofunctionalization. The installation of IL-like units in the cellulose matrix was achieved by quaternization of 1-*N*-ferrocenylmethyl benzimidazole (**6**) with **5** to yield a heterogeneous azolium salt given the acronym [CellFemBenz]Cl (**7**), which on further treatment with NH_4OH formed [CellFemBenz]OH (**8**). Finally, the anion metathesis reaction of **8** with (±)-10-camphorsulfonic acid (CSA) (**9**) resulted in the formation of the desired cellulose-SILP catalyst containing camphor sulfonate with a pendant ferrocenyl group, denoted [CellFemBenz]CSA (**10**).

Fourier-transform (FT) Raman and FT-infrared (FT-IR) spectroscopy were used to monitor the progress of reactions involved in the preparation of [CellFemBenz]CSA (**10**). The reaction of **3** with **4** was monitored by FT-Raman spectroscopy. The characteristic vibrations at 1293 cm^{-1} (wagging vibrations of CH_2–Cl), 1094 cm^{-1} (Si–O–C stretching vibrations), and 610 cm^{-1} (C–Cl stretching vibrations) indicate the formation of **5**. Furthermore, the FT-IR spectrum of **5** displayed characteristic peaks at

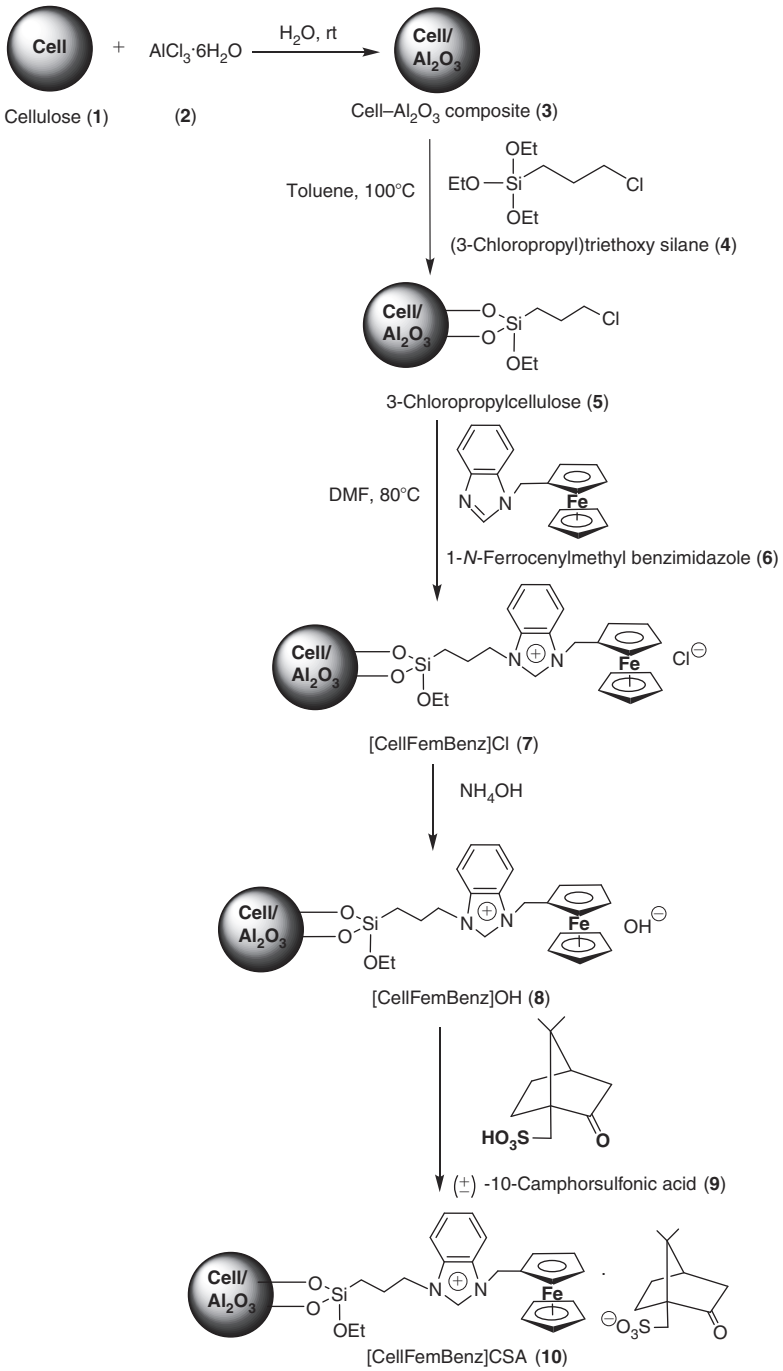

Scheme 1. Preparation of [CellFemBenz]CSA (**10**).

1341 cm^{-1} (C–O stretching vibrations), 1175 cm^{-1} (Si–O stretching vibrations), 987 cm^{-1} (C–C aliphatic stretching vibrations), 891 cm^{-1} (Si–C stretching vibrations), and 702 cm^{-1} (C–Cl stretching vibrations) confirming the formation of **5**. The formation of [CellFemBenz]Cl (**7**) was monitored by FT-Raman spectroscopy. The peaks at 3145 and 3108 cm^{-1} (C–H stretching vibrations of cyclopentadienyl (Cp) rings), 1470, 1410, 1335, and 1256 cm^{-1} (ring stretching modes of benzimidazolium ring), and 460 cm^{-1} (Fe–Cp stretching vibrations) reflect successful installation of the IL-like unit in the cellulose matrix of **5**. This was further confirmed by the FT-IR spectrum of **7**, which displayed characteristic peaks at 1634 cm^{-1} (C=C stretching vibrations of benzimidazolium ring), 1428 cm^{-1} (C–N stretching vibrations of benzimidazolium ring), 2898, 1366, 1336, 1317 cm^{-1} (Cp ring stretching vibrations), and 471 cm^{-1} (Cp–Fe stretching vibrations). The anion metathesis of **7** with NH_4OH to form [CellFemBenz]OH (**8**) was monitored by FT-Raman spectroscopy. The appearance of the characteristic stretching band of medium intensity of the O–H group at 3432 cm^{-1} revealed the replacement of Cl^- by OH^-. In addition, the FT-IR spectrum of **8** displayed a characteristic peak at 3349 cm^{-1} (O–H stretching vibrations) confirming its formation. The formation of [CellFemBenz]CSA (**10**) was monitored by FT-Raman spectroscopy, which displayed characteristic bands at 1744 cm^{-1} (C=O stretching), 1092 cm^{-1} (S–O stretching), and 703 cm^{-1} (C–S aliphatic stretching). The formation of **10** was further confirmed from the FT-IR spectrum, which displayed characteristic peaks at 1746 cm^{-1} (C=O stretching vibrations of camphor sulfonate anion), 716 cm^{-1} (C–S stretching vibrations of camphor sulfonate anion), 1009 cm^{-1} (S–O stretching vibrations of camphor sulfonate anion), and 2898 cm^{-1} (C–H stretching vibrations of CH_3 group). Additionally, the cross polarization–magic angle spinning (CP-MAS) ^{13}C NMR spectrum of [CellFemBenz]CSA (**10**) displayed peaks at 155 ppm (C_1 of benzimidazolium), 145 ppm (C_2 and C_7 of benzimidazolium), 110 ppm (C_4 and C_5 of benzimidazolium), 107 ppm (C_3 and C_6 of benzimidazolium), 90 ppm (broad singlet, C_1 of cellulose), 83 ppm (singlet, substituted Cp ring carbon of ferrocene), 75–72 ppm (multiplet, C_2, C_3, C_4, C_5, C_6 of cellulose), and 68 ppm (singlet, non-substituted Cp ring carbon of ferrocene) confirming the proposed structure of **10**.

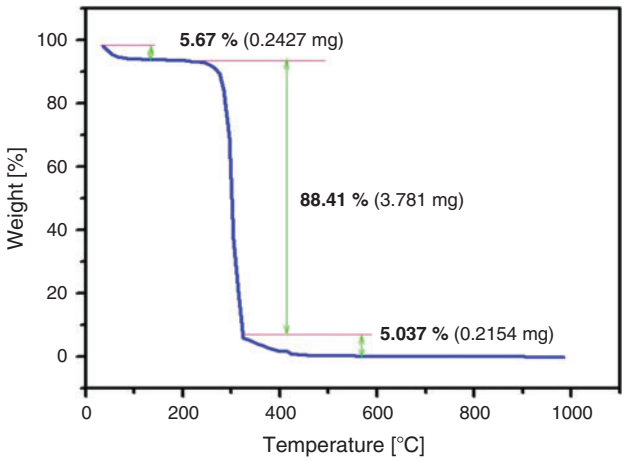

Fig. 1. Thermogravimetric analysis (TGA) curve for [CellFemBenz]CSA (**10**).

Energy-dispersive X-ray spectroscopy (EDX) and elemental analysis were used for quantification of the camphor sulfonate anion in [CellFemBenz]CSA (**10**). Elemental analysis revealed the presence of 0.077 mmol of camphor sulfonate anion g^{-1} of **10**.

The thermal profile of [CellFemBenz]CSA (**10**) was studied using thermogravimetric analysis (TGA) in the temperature range 25–1000°C (Fig. 1). The thermogram of **10** displayed an initial weight loss of 5.6 % below 100°C due to the evaporation of physically adsorbed water. The second major weight loss of 88.4 % up to 324 °C is ascribed to the combined weight loss of the pendant ferrocenyl group and other organic scaffolds from the cellulose matrix. The consequent weight loss of 5.0 % is attributed to the decomposition of cellulose units through the formation of volatile compounds. The observations are in good agreement with the TGA profile of cellulose reported in the literature.[48,49]

To investigate morphological changes on the surface of the cellulose support at various stages of preparation of the SILP catalyst, field emission-scanning electron microscopy (FE-SEM) was employed. The SEM images of cellulose (**1**), [CellFemBenz]Cl (**7**), [CellFemBenz]OH (**8**), and [CellFemBenz]CSA (**10**) are displayed in Fig. 2a–d. The images show no alteration in the morphology of the cellulose support. The fibrous morphology of cellulose, with diameters in the range of several hundred micrometres, was retained even after multistep synthesis, revealing the effectiveness of cellulose as a support in the preparation of the SILP catalyst.

Evidence for the retention of the microcrystalline nature of cellulose (**1**) in [CellFemBenz]CSA (**10**) was investigated by X-ray diffraction (XRD) analysis. The characteristic diffraction peaks in the diffractogram indexed to the microcrystalline

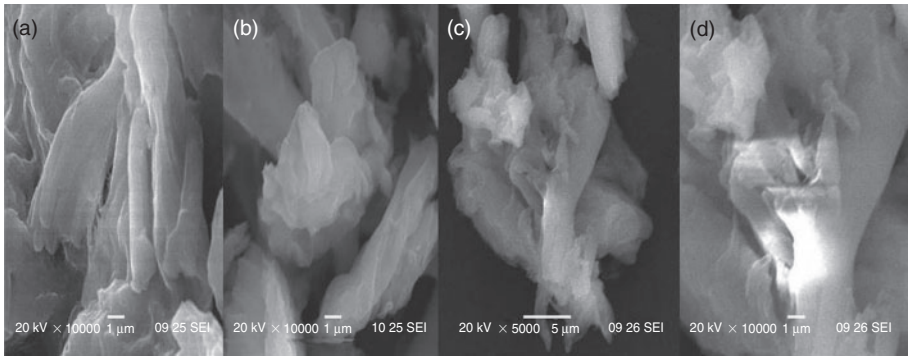

Fig. 2. SEM images of (a) cellulose (**1**); (b) [CellFemBenz]Cl (**7**); (c) [CellFemBenz]OH (**8**); and (d) [CellFemBenz]CSA (**10**).

nature of **1** (Fig. 3). The characteristic peaks at 2θ values of 15.06° and 22.48° being assigned to the reflections (1 0 1), (0 0 2) by virtue of transverse arrangement of the crystallites in **1**. A pronounced peak at a 2θ value of 34.25° correlates to the (0 4 0) reflection, which is attributed to the longitudinal structure of the polymer. Thus, XRD analysis revealed preservation of the microcrystalline structure of **1** in **10** even after multistep functionalization.[50]

Our next task was to investigate the catalytic potential of [CellFemBenz]CSA (**10**) in the Mannich reaction. In order to optimize reaction parameters, the reaction between acetophenone (**11a**), benzaldehyde (**12a**), and aniline (**13a**) was chosen as a model reaction. Initially, the effect of various solvents on the model reaction was studied, and results are summarised in Table 1. Ethanol was found to be the most effective solvent, providing the highest yield of 1,3-diphenyl-3-(phenylamino) propan-1-one (Table 1, entry 4). In contrast, solvent-free conditions as well as solvents such as H_2O, MeOH, CH_2Cl_2, CH_3CN, THF, DMF, toluene, and $CHCl_3$ resulted in comparatively lower yields (Table 1, entries 1–3, 5–10).

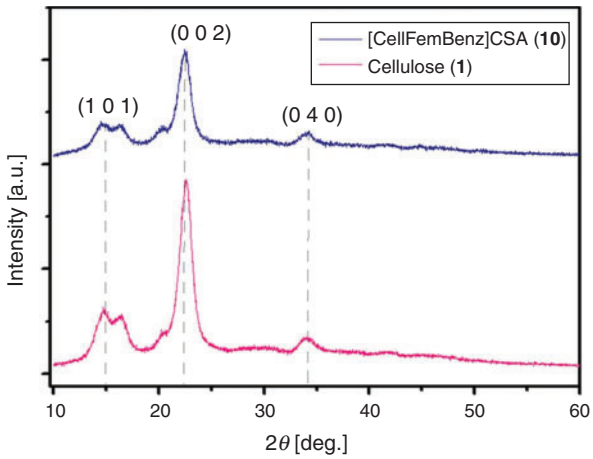

Fig. 3. XRD of cellulose (**1**) and [CellFemBenz]CSA (**10**).

Next, the effect of catalytic loading was investigated. The model reaction was tested by varying the amount of **10** in ethanol at ambient temperature and the results are summarised in Table 2. In the absence of catalyst, reaction did not proceed even after a prolonged reaction time of 24 h (Table 2, entry 1), whereas in the presence of **10**, a significant improvement in the yield of corresponding product **14a** was observed. It was found that 0.05 g of **10** was sufficient to efficiently drive the model reaction to afford the desired product in excellent yield (92 %) within 5 h (Table 2, entry 6). Further, we noted that amounts less than 0.05 g gave lower yields (Table 2, entries 1–5), whereas increasing the catalyst quantity beyond this value did not lead to any significant improvement in the yield (Table 2, entries 7–9).

The next parameter investigated was the reaction temperature (Table 2). The model reaction performed in ethanol with 0.05 g of **10** at room temperature gave the best result (Table 2, entry 6). No improvement in the yield of product was observed when the reaction temperature was increased (Table 2, entries 10–13). Thus, 0.05 g of catalyst, ethanol as solvent, and room temperature were selected as optimum reaction conditions for further studies.

After the optimization of reaction conditions, the generality of the protocol was investigated by reacting structurally diverse aldehydes, amines, and acetophenones. The results summarised in Table 3 indicate that the electronic effect of substituents on the reactants has a significant impact on the yield of products. It is seen that electron-donating groups on ketones resulted in better yields (Table 3, entries 11b, c) as compared with electron-withdrawing groups (Table 3, entry 11e). Further, the electron-donating group-substituted amines afforded the corresponding products in better yields than electron-withdrawing group-substituted amines (Table 3, entries 11j and 11i). Moreover, the reaction was found to be sensitive to steric hindrance as well as electronic effect of the substituents. Orthosubstituted reactants produced moderate yields of corresponding product owing to the steric effect (Table 3, entries 11d, 13g, and 13k).

A plausible mechanism for the [CellFemBenz]CSA (**10**) catalyzed Mannich reaction is depicted in Scheme 2 and is based on the report by Ishikawa et al.[51] The presence of the bulky camphor sulfonate anion and cylindrical ferrocenyl

Table 1. Optimization of solvent in [CellFemBenz]CSA (10)-catalyzed Mannich reaction[A]

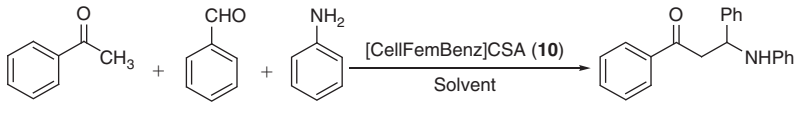

11a **12a** **13a** **14a**

Entry	Solvents	Yield[B] [%]
1	Solvent-free	67
2	H_2O	74
3	MeOH	81
4	EtOH	92
5	CH_2Cl_2	62
6	CH_3CN	72
7	THF	48
8	DMF	51
9	Toluene	Trace
10	$CHCl_3$	57

[A]Reaction conditions: acetophenone (1 mmol), benzaldehyde (1 mmol), aniline (1 mmol), [CellFemBenz]CSA (0.05 g), solvent (5 mL), rt, 5 h.
[B]Isolated yields after chromatography.

group[52–57] on the cation in **10** results in weaker coulombic interactions between cation and anion. This keeps the cation and anion as far as away from each other. Further, as the solvent used for this reaction is ethanol, which is polar, it is capable of solvating the hydrophobic camphor sulfonate anion, which is already at a distance from the cation owing to its bulky nature. This frees the [CellFemBenz] cation. This facilitates favourable H-bonding interaction between the proton of C_2 of the benzimidazolium cation in **10** and the carbonyl group of the aldehyde (**III**). This assists the nucleophilic attack of the amine **II** on the activated aldehyde **III** to form the iminium cation **IV**. Further, the enol **V** formed via tautomerization of ketone **I** reacts with **IV**, furnishing the desired product **VI**. The proposed mechanism is supported by the fact that when [CellFemBenz]Cl (**7**) and [CellFemBenz]OH (**8**) were used as catalysts, the model reaction did not proceed to a synthetically useful degree as the yield of corresponding product was 52 and 61 % respectively, indicating the role of the camphor sulfonate anion is important.

To confirm the heterogeneity of [CellFemBenz]CSA (**10**), a hot filtration test was carried out for the model reaction. After 50 % conversion (by gas chromatography), the reaction mixture was split into two parts by simple filtration, and both reaction mixtures were stirred for an additional 3 h. The mixture containing **10** proceeded to completion whereas the other portion without **10** did not show any increase in the yield of product beyond 50 % (**14a**). This indicates that almost all IL-like units containing the camphor sulfonate anion are significantly embedded in the crystalline framework of the cellulose support, thereby making the catalyst leaching-resistant for good regeneration and reusability.

The recyclability and reusability of [CellFemBenz]CSA (**10**) were investigated for the model reaction under the optimized reaction conditions. On completion of the reaction, the catalyst was filtered, washed with copious amount of ethanol to remove any adhering reactants, and dried at 60°C under vacuum for 1 h. The recovered catalyst was reused for six subsequent runs without noticeable drop in product yield and catalytic activity (Fig. 4).

It is noteworthy that the FT-Raman spectra of both fresh and reused [CellFemBenz]CSA (**10**) revealed the same functional groups even after six successive cycles. Further, EDX analysis of reused catalyst indicated no significant difference in composition in comparison with the fresh catalyst. Moreover, the SEM images of both fresh and reused catalysts (Fig. 5a, b) indicates that the morphology of the catalyst is preserved after six successive runs. The results reveal that **10** is stable and does not undergo physical or chemical changes during recycling and after multiple reuse.

To demonstrate the merits of the present protocol, we compared the efficiency of [CellFemBenz]CSA **(10)** with some of the reported catalysts used in the synthesis of 1,3-diphenyl-3-(phenylamino)propan-1-one (**14a**) by Mannich reaction between acetophenone (**11a**), benzaldehyde (**12a**), and aniline (**13a**). The results are summarised in Table 4. It is evident that **10** is superior to many of the reported catalysts with respect to either loading, temperature, time, or yield of the product.

Conclusion

Cellulose SILP catalyst containing a camphor sulfonate anion with a pendant ferrocenyl group was prepared and its catalytic efficiency evaluated in the synthesis of β-amino carbonyl compounds via Mannich reactions of aldehydes, amines, and acetophenones. The present strategy offers several key features such as low catalyst loading, remarkable catalytic performance, ability to work at ambient temperature, flexibility in the synthesis, clean reaction profile, easy work-up procedure, and facile recyclability and reusability of catalyst. Studies aimed at extending the scope of the cellulose SILP catalyst containing a camphor sulfonate anion for other organic transformations are currently under way in our laboratory.

Experimental

General Remarks

All the starting reagents, solvents, and cellulose were of standard analytical grade, purchased from local suppliers, and used

Table 2. Optimization of catalyst loading in [CellFemBenz]CSA (10)-promoted Mannich reaction[A]

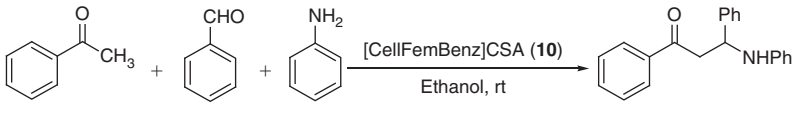

11a **12a** **13a** **14a**

Entry	Catalyst [g]	Temperature [°C]	Time [h]	Yield[B] [%]
1	No catalyst	rt	24.0	None
2	0.01	rt	7.5	56
3	0.02	rt	7.0	69
4	0.03	rt	6.5	76
5	0.04	rt	5.5	83
6	0.05	rt	5.0	92
7	0.06	rt	5.0	93
8	0.07	rt	4.5	94
9	0.08	rt	4.0	94
10	0.05	40	4.5	93
11	0.05	50	4.0	93
12	0.05	60	3.5	94
13	0.05	80	3.5	94

[A]Reaction conditions: acetophenone (1 mmol), benzaldehyde (1 mmol), aniline (1 mmol), ethanol (5 mL), rt.
[B]Isolated yields after chromatography.

Table 3. [CellFemBenz]CSA (10)-catalyzed synthesis of β-amino carbonyl compounds[A]

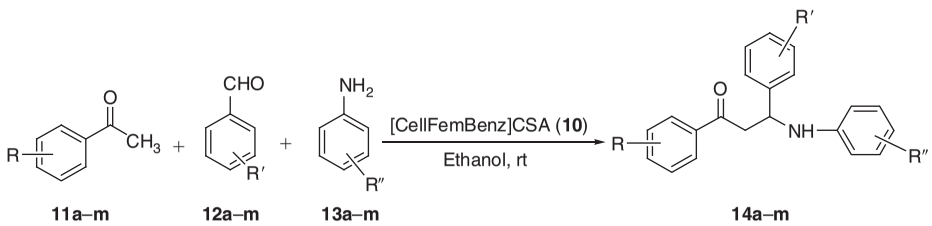

Entry	Ketone (**11**)	Aldehyde (**12**)	Amine (**13**)	Product (**14**)	Time [h]	Yield[B] [%]
a	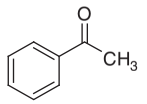	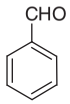	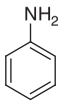	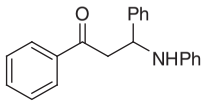	5	92
b	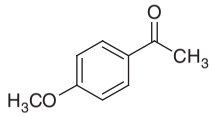	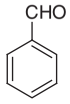	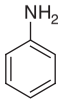	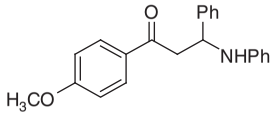	9	82
c	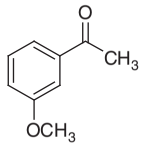	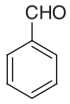	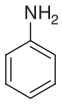	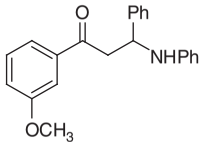	10	79
d	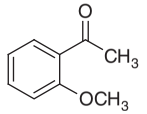	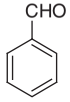	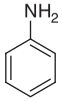	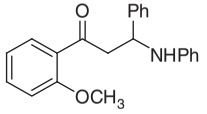	11	70
e	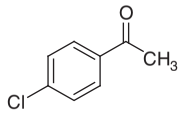	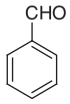	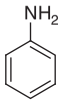	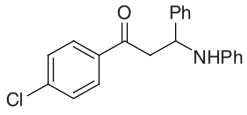	8	72
f	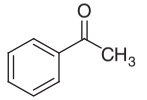	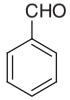	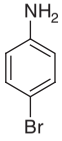	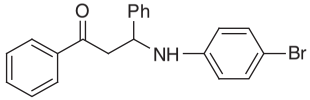	9	74

g	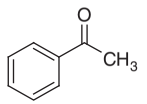	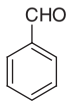	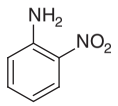	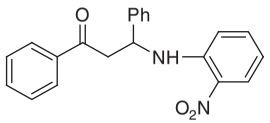	15	69
h	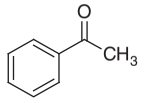	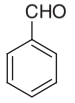	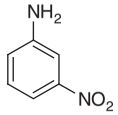	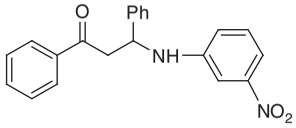	5.5	89
i	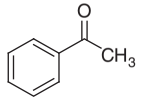	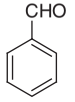	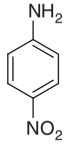	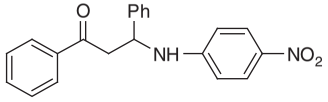	6	78
j	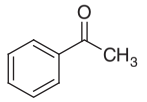	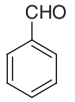	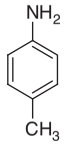	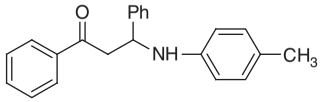	15	84
k	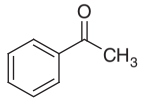	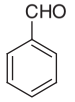	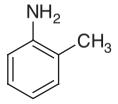	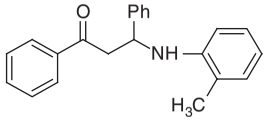	7.3	76
l	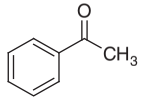	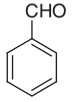	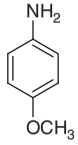	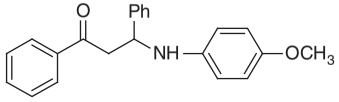	8	73
m	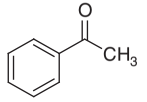	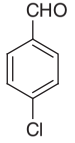	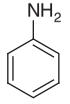	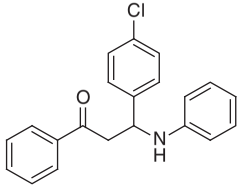	3.5	94

[A]Reaction conditions: acetophenone (1 mmol), aldehyde (1 mmol), amine (1 mmol), [CellFemBenz]CSA (0.05 g), ethanol (5 mL), rt.
[B]Isolated yields after chromatography.

without further purification. (±)-10-Camphorsulfonic acid was purchased from Sigma–Aldrich Co. and was used as received. All reactions were carried out under air in dried glassware. Infrared spectra were measured with a PerkinElmer One FT-IR spectrophotometer. The samples were examined as ~5 % w/w KBr discs. Raman spectroscopy was carried out using a Bruker FT-Raman MultiRAM spectrometer. The elemental composition of materials was analysed by EDS attached to a field-emission scanning electron microscope (Hitachi S 4800). ^{1}H and ^{13}C NMR spectra were recorded on a Bruker AC (300 MHz for ^{1}H NMR and 75 MHz for ^{13}C NMR) spectrometer using $CDCl_3$ as solvent and tetramethylsilane (TMS) as internal standard. Chemical shifts, δ, are expressed in parts per million (ppm) and coupling constants are expressed in hertz (Hz). The CP-MAS ^{13}C NMR spectrum was recorded with a Jeol-ECX400 type FT-NMR spectrometer under prescribed operating conditions. Mass spectra were recorded on a Shimadzu QP2010 GCMS. The materials were analysed by SEM using a Jeol JSM with 5 and 20 kV accelerating voltage. Melting points were determined on a MEL-TEMP capillary melting point apparatus and are uncorrected. 1-*N*-Ferrocenylmethyl benzimidazole was synthesised following the literature procedure.[58]

*Preparation of Cell–Al_2O_3 Composite (**3**)*

A mixture of microcrystalline cellulose (**1**) (15 g) and aluminium chloride hexahydrate (**2**) (15 g) in water (200 mL) was stirred for 12 h. Then, the mixture was filtered, and the residue was exposed to ammonia. It was then washed with water and dried under vacuum at room temperature to get the Cell–Al_2O_3 composite (**3**). By calcining **2** (0.300 g) at 600°C for 8 h, the amount of aluminium was determined and the residue, weighed as Al_2O_3, was found to be 3.28 wt-%, corresponding to 0.69 mmol aluminium g^{-1} of **3**.

*Preparation of Chloropropyl Cellulose (**5**)*

A mixture of **3** (10.0 g) and (3-chloropropyl)triethoxysilane (**4**) (9.6 mL, 40.0 mmol) in toluene (10 mL) was refluxed in an oil bath for 24 h. The reaction mixture was cooled, filtered, and the product was washed with toluene (3 × 5 mL) and dried under

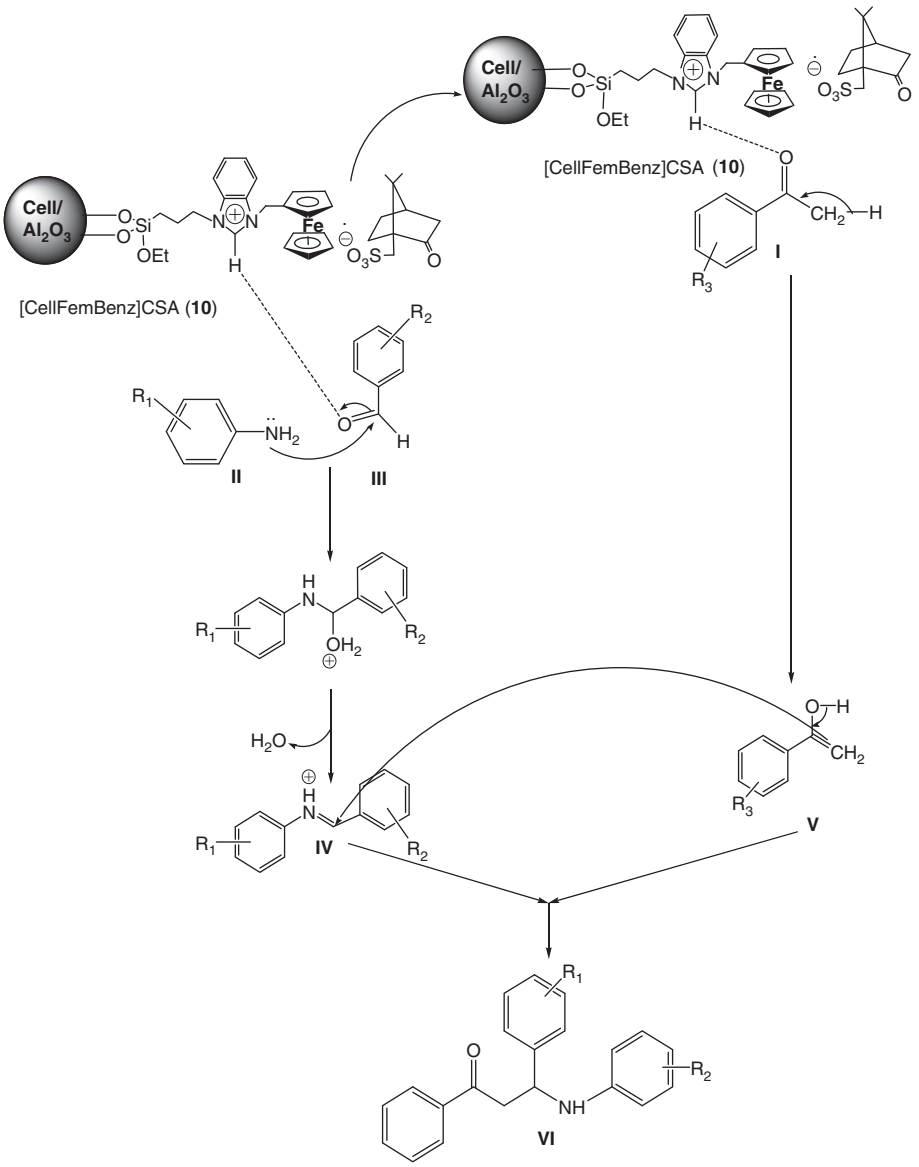

Scheme 2.

vacuum at room temperature for 8 h to afford chloropropyl cellulose (**5**). FT-IR ν_{max} (KBr, thin film)/cm^{-1} 3345, 2906, 1635, 1426, 1341, 1175, 1171, 987, 891, 702, 579. Raman ν_{max} (KBr)/cm^{-1} 2898, 1481, 1375, 1293, 1117, 1094, 898, 610, 519, 381. Elemental analysis found (%): C 73.00, O 23.07, Al 1.84, Cl 2.09 %. Loading: 0.59 mmol functional group g^{-1} of **5**.

*Preparation of [CellFemBenz]Cl (**7**)*

A mixture of **5** (7.0 g) and 1-*N*-ferrocenylmethyl benzimidazole (**6**) (4.3 g, 10 mmol) in DMF (25 mL) was heated at 80°C in an oil bath for 72 h. The solid was filtered, washed with DMF (3 × 50 mL), MeOH (3 × 50 mL), and CH_2Cl_2 (3 × 50 mL), and dried under vacuum at 50°C for 24 h to produce **7**. FT-IR ν_{max} (KBr, thin film)/cm^{-1} 2898, 1634, 1428, 1366, 1336, 1317, 1163, 471. Raman ν_{max}/cm^{-1} 3145, 3108, 1637, 1578, 1470, 1410, 1335, 1256, 1157, 775, 710, 645, 521, 460. Anal. found: C 39.68, N 1.59, H 5.90 %. Loading: 0.56 mmol benzimidazolium units g^{-1} of **7**.

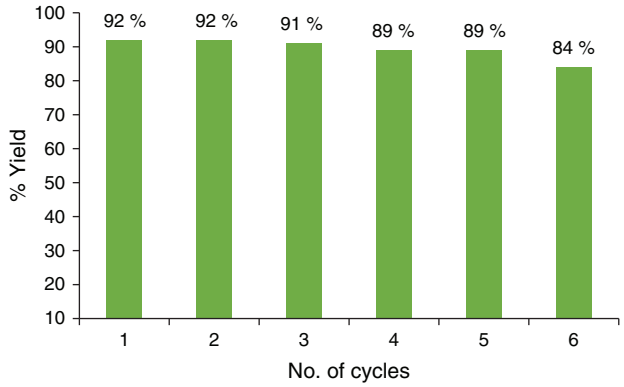

Fig. 4. Recyclability study of [CellFemBenz]CSA (**10**) in the synthesis of 1,3-diphenyl-3-(phenylamino)propan-1-one (**14a**).

*Preparation of [CellFemBenz]OH (**8**)*

A mixture of **7** (5.0 g) and an aqueous solution of NH_3 (30 mL) was stirred for 48 h at room temperature. Afterwards, the solid was filtered and washed with MeOH (3 × 20 mL), MeOH/H_2O (1 : 1) (3 × 20 mL), H_2O (3 × 20 mL), and MeOH (3 × 20 mL), and then dried under vacuum at 50°C for 48 h to get [CellFemBenz]OH (**8**). The quantification of hydroxyl groups in **8** was carried out by volumetric titration [59,60] and was found to be 0.23 mmol g^{-1} of **8**. FT-IR ν_{max} (KBr, thin film)/cm^{-1} 3349, 2905, 1634, 1432, 1360, 1317, 1162, 1105, 1027, 605. Raman ν_{max} (KBr)/cm^{-1} 3432, 3110, 1744, 1640, 1578, 1472, 1410, 1335, 1260, 1160, 776, 710, 703, 521, 460. Anal. found: C 61.29, N 0.90, Al 1.19, Si 0.24, Fe 0.27 %. Loading: 0.23 mmol OH groups g^{-1} of **8**.

*Preparation of [CellFemBenz]CSA (**10**)*

[CellFemBenz]OH (3.0 g) was stirred in (±)-CSA (**9**) (0.05 M, 50 mL) at room temperature for 48 h. Afterwards, the mixture was filtered and the residue was washed with CH_2Cl_2 (3 × 20 mL) and H_2O (3 × 20 mL), and dried under vacuum for 48 h to afford [CellFemBenz]CSA complex (**10**). FT-IR ν_{max} (KBr, thin film)/cm^{-1} 3373, 2898, 2829, 2115, 1746, 1645,

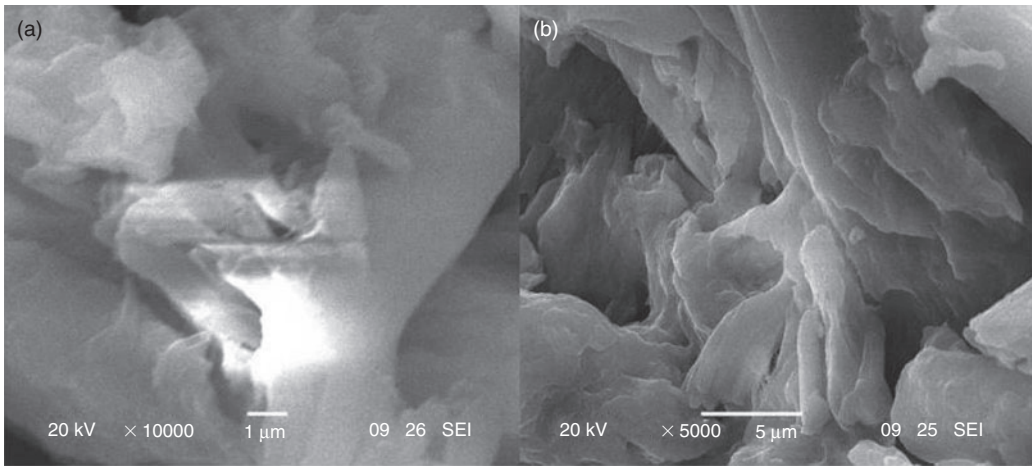

Fig. 5. FE-SEM images of (a) fresh [CellFemBenz]CSA (**10**); and (b) reused [CellFemBenz]CSA (**10**).

Table 4. Comparative studies of [CellFemBenz]CSA (10) in the synthesis of 14a

Entry	Catalyst	Amount of catalyst	Temperature [°C]	Time [h]	Yield [%]	Ref.
1	CFPIL-1	0.032 g	rt	5	70	[38]
2	PS-SO_3H	0.080 g	30°C	24	75	[39]
3	Yttria–zirconia-based Lewis acid	10 mol-%	65°C	10	83	[40]
4	$H_3PW_{12}O_{40}$	0.691 g	rt	18	76	[41]
5	Carbon-based solid acid	0.10 g	rt	3.45	90	[42]
6	$BiCl_3$	5 mol-%	rt	11	95	[43]
7	(±)-10-Camphorsulfonic acid	5 mol-%	rt	4	88	[61]
8	[CellFemBen]CSA/EtOH	1.63 mol-%	rt	5	92	Present work

1434, 1009, 716. Raman ν_{max} (KBr)/cm^{-1} 3110, 2890, 1745, 1619, 1577, 1480, 1410, 1256, 1092, 779, 703, 645, 521, 465. Anal found: C 37.81, H 5.63, N 0.23, S 0.58. Loading: 0.077 mmol of camphor sulfonate anion g^{-1} of **10**.

General Procedure for the Synthesis of β-Amino Carbonyl Compounds

A mixture of aldehyde (1 mmol), aniline (1 mmol), acetophenone (1 mmol), and [CellFemBenz]CSA (**10**) (0.05 g) was stirred in ethanol (5 mL) at ambient temperature for the appropriate time indicated in Table 3. On completion of the reaction as monitored by TLC, the reaction mixture was filtered to recover the insoluble catalyst. The reaction mixture was then evaporated at room temperature (rt). The resulting crude product was washed with ethanol and purified by column chromatography over silica gel using 10 % ethyl acetate and 90 % light petroleum as an eluent to yield pure β-amino carbonyl compounds.

Supplementary Material

Spectral data of synthesised β-amino carbonyl compounds are available on the Journal's website.

Conflicts of Interest

The authors declare no conflicts of interest.

Acknowledgements

We gratefully acknowledge the Indian Institute of Sciences (IISc), Bangalore, and Sophisticated Analytical Instrumental Facility, Indian Institute of Technology, Madras (IITM), for providing spectral facilities. This research did not receive any specific funding.

References

[1] T. Welton, *Chem. Rev.* **1999**, *99*, 2071. doi:10.1021/CR980032T
[2] C. P. Mehnert, R. A. Cook, N. C. Dispenziere, M. Afeworki, *J. Am. Chem. Soc.* **2002**, *124*, 12932. doi:10.1021/JA0279242
[3] B. Xin, J. Hao, *Chem. Soc. Rev.* **2014**, *43*, 7171. doi:10.1039/C4CS00172A
[4] M. Mirzaei, A. Badiei, B. Mokhtarani, A. Sharifi, *J. Mol. Liq.* **2017**, *232*, 462. doi:10.1016/J.MOLLIQ.2017.02.104
[5] N. Gathergood, P. J. Scammells, *Aust. J. Chem.* **2002**, *55*, 557. doi:10.1071/CH02148
[6] C. Van Doorslaer, J. Wahlen, P. Mertens, K. Binnemans, D. De Vos, *Dalton Trans.* **2010**, *39*, 8377. doi:10.1039/C001285H
[7] A. Riisager, R. Fehrmann, M. Haumann, P. Wasserscheid, *Top. Catal.* **2006**, *40*, 91. doi:10.1007/S11244-006-0111-9
[8] P. Sharma, M. Gupta, M. Gupta, R. Gupta, *Aust. J. Chem.* **2016**, *69*, 230. doi:10.1071/CH15133
[9] A. Riisager, R. Fehrmann, M. Haumann, P. Wasserscheid, *Eur. J. Inorg. Chem.* **2006**, 695. doi:10.1002/EJIC.200500872
[10] M. Zhang, Q. Sun, Z. Yan, J. Jing, W. Wei, D. Jiang, J. Xie, M. Chen, *Aust. J. Chem.* **2013**, *66*, 564. doi:10.1071/CH12484
[11] H. Li, P. S. Bhadury, B. Song, S. Yang, *RSC Adv.* **2012**, *2*, 12525. doi:10.1039/C2RA21310A
[12] M. I. Burguete, H. Erythropel, E. Garcia-Verdugo, S. V. Luis, V. Sans, *Green Chem.* **2008**, *10*, 401. doi:10.1039/B714977H
[13] M. A. Gelesky, S. S. X. Chiaro, F. A. Pavan, J. H. Z. dos Santos, J. Dupont, *Dalton Trans.* **2007**, 5549. doi:10.1039/B708111A
[14] T. Takeshita, A. Kitagawa, F. Yokosu, R. Matsumoto, T. Nokami, T. Itoh, *Aust. J. Chem.* **2019**, *72*, 61. doi:10.1071/CH18253
[15] G. Rashinkar, R. Salunkhe, *J. Mol. Catal. Chem.* **2010**, *316*, 146. doi:10.1016/J.MOLCATA.2009.10.013
[16] R.-Q. Yang, N. Zhang, X.-G. Meng, X.-H. Liao, L. Li, H.-J. Song, *Aust. J. Chem.* **2018**, *71*, 559. doi:10.1071/CH18138
[17] V. Sans, N. Karbass, M. I. Burguete, V. Compan, E. Garcia-Verdugo, S. V. Luis, M. Pawlak, *Chem. – Eur. J.* **2011**, *17*, 1894. doi:10.1002/CHEM.201001873
[18] D. Kale, G. Rashinkar, A. Kumbhar, R. Salunkhe, *React. Funct. Polym.* **2017**, *116*, 9. doi:10.1016/J.REACTFUNCTPOLYM.2017.04.010
[19] M. Jagadale, S. Khanapure, R. Salunkhe, M. Rajmane, G. Rashinkar, *Appl. Organomet. Chem.* **2016**, *30*, 125. doi:10.1002/AOC.3407
[20] A. Rahmatpour, *React. Funct. Polym.* **2011**, *71*, 80. doi:10.1016/J.REACTFUNCTPOLYM.2010.11.001
[21] L. Rodríguez-Pérez, E. Teuma, A. Falqui, M. Gómez, P. Serp, *Chem. Commun.* **2008**, 4201. doi:10.1039/B804969F
[22] J.-P. Mikkola, P. Virtanen, H. Karhu, T. Salmi, D. Y. Murzin, *Green Chem.* **2006**, *8*, 197. doi:10.1039/B508033A
[23] N. Clousier, R. Moucel, P. Naik, P.-J. Madec, A. C. Gaumont, I. Dez, *C. R. Chim.* **2011**, *14*, 680. doi:10.1016/J.CRCI.2010.08.004
[24] Y. Qiao, H. Li, L. Hua, L. Orzechowski, K. Yan, B. Feng, Z. Pan, N. Theyssen, W. Leitner, Z. Hou, *ChemPlusChem* **2012**, *77*, 1128. doi:10.1002/CPLU.201200246
[25] L. Berglund, A. Bismarck, A. Dufresne, A. Isogai, *React. Funct. Polym.* **2014**, *85*, 77. doi:10.1016/J.REACTFUNCTPOLYM.2014.11.005
[26] M. Sharifi, S.-M. Robatjazi, M. Sadri, J. M. Mosaabadi, *React. Funct. Polym.* **2018**, *124*, 162. doi:10.1016/J.REACTFUNCTPOLYM.2018.01.019
[27] D. Fenn, M. Pohl, T. Heinze, *React. Funct. Polym.* **2009**, *69*, 347. doi:10.1016/J.REACTFUNCTPOLYM.2009.02.007
[28] X. Chen, J. Chen, T. You, K. Wang, F. Xu, *Carbohydr. Polym.* **2015**, *125*, 85. doi:10.1016/J.CARBPOL.2015.02.054
[29] A. Mohammadinezhad, M. A. Nasseri, M. Salimi, *RSC Adv.* **2014**, *4*, 39870. doi:10.1039/C4RA06450J
[30] A. Shaabani, Z. Hezarkhani, S. Shaabani, *RSC Adv.* **2014**, *4*, 64419. doi:10.1039/C4RA11101J
[31] D. Baruah, U. P. Saikia, P. Pahari, D. K. Dutta, D. Konwar, *RSC Adv.* **2014**, *4*, 59338. doi:10.1039/C4RA08803D
[32] F. Quignard, A. Choplin, *Chem. Commun.* **2001**, 21. doi:10.1039/B007776N
[33] Y. Habibi, L. A. Lucia, O. J. Rojas, *Chem. Rev.* **2010**, *110*, 3479. doi:10.1021/CR900339W
[34] C. Tsioptsias, A. Stefopoulos, I. Kokkinomalis, L. Papadopoulou, C. Panayiotou, *Green Chem.* **2008**, *10*, 965. doi:10.1039/B803869D
[35] R. Müller, H. Goesmann, H. Waldmann, *Angew. Chem. Int. Ed.* **1999**, *38*, 184. doi:10.1002/(SICI)1521-3773(19990115)38:1/2<184::AID-ANIE184>3.0.CO;2-E
[36] K. Mogilaiah, G. Kankaiah, *Indian J. Heterocycl. Chem.* **2002**, *11*, 283.
[37] F. A. Davis, M. B. Nolt, Y. Wu, K. R. Prasad, D. Li, B. Yang, K. Bowen, S. H. Lee, J. H. Eardley, *J. Org. Chem.* **2005**, *70*, 2184. doi:10.1021/JO0402780
[38] A. G. Khiratkar, K. R. Balinge, K. J. Bhansali, P. R. Bhagat, *Res. Chem. Intermed.* **2018**, *44*, 787. doi:10.1007/S11164-017-3134-X
[39] A. Davoodnia, A. Tavakoli-Nishaburi, N. Tavakoli-Hoseini, *Bull. Korean Chem. Soc.* **2011**, *32*, 635. doi:10.5012/BKCS.2011.32.2.635
[40] H. Li, H.-Y. Zeng, H.-W. Shao, *Tetrahedron Lett.* **2009**, *50*, 6858. doi:10.1016/J.TETLET.2009.09.131
[41] S. Iimura, D. Nobutou, K. Manabe, S. Kobayashi, *Chem. Commun.* **2003**, 1644. doi:10.1039/B304343F
[42] S. Ramalingam, P. Kumar, *Catal. Commun.* **2008**, *9*, 2445. doi:10.1016/J.CATCOM.2008.06.011
[43] N. Azizi, L. Torkiyan, M. R. Saidi, *Org. Lett.* **2006**, *8*, 2079. doi:10.1021/OL060498V
[44] R. Kurane, J. Jadhav, S. Khanapure, R. Salunkhe, G. Rashinkar, *Green Chem.* **2013**, *15*, 1849. doi:10.1039/C3GC40592C
[45] A. Naikwade, M. Jagadale, D. Kale, S. Gajare, G. Rashinkar, *Catal. Lett.* **2018**, *148*, 3178. doi:10.1007/S10562-018-2514-1
[46] U. P. R. Filho, Y. Gushikem, F. Y. Fujiwara, S. C. de Castro, I. C. L. Torriani, L. P. Cavalcanti, *Langmuir* **1994**, *10*, 4357. doi:10.1021/LA00023A070
[47] A. Bhattacharya, B. N. Misra, *Prog. Polym. Sci.* **2004**, *29*, 767. doi:10.1016/J.PROGPOLYMSCI.2004.05.002

[48] Y. Wu, Z. Fu, D. Yin, Q. Xu, F. Liu, C. Lu, L. Mao, *Green Chem.* **2010**, *12*, 696. doi:10.1039/B917807D
[49] O. W. Guirguis, M. T. H. Moselhey, *Nat. Sci.* **2012**, *4*, 57.
[50] M. Sevilla, A. B. Fuertes, *Carbon* **2009**, *47*, 2281. doi:10.1016/J.CARBON.2009.04.026
[51] K. Nobuoka, S. Kitaoka, K. Kunimitsu, M. Iio, T. Harran, A. Wakisaka, Y. Ishikawa, *J. Org. Chem.* **2005**, *70*, 10106. doi:10.1021/JO051669X
[52] *Metallocenes* (Eds A. Togni, R. L. Halterman) **1998** (Wiley-VCH, Verlag GmbH: Weinheim).
[53] *Ferrocenes: Homogeneous Catalysis, Organic Synthesis, Material Science* (Eds A. Togni, T. Hayashi) **1995** (Wiley-VCH, Verlag GmbH: Weinheim).
[54] R. C. Atkinson, V. C. Gibson, N. J. Long, *Chem. Soc. Rev.* **2004**, *33*, 313. doi:10.1039/B316819K
[55] P. Barbaro, C. Bianchini, G. Gianbastini, S. L. Parisel, *Coord. Chem. Rev.* **2004**, *248*, 2131. doi:10.1016/J.CCR.2004.03.022
[56] U. Siemeling, T.-C. Auch, *Chem. Soc. Rev.* **2005**, *34*, 584. doi:10.1039/B315486F
[57] T. J. Colacot, *Platin. Met. Rev.* **2001**, *45*, 22.
[58] Y. Gao, B. Twamley, J. M. Shreeve, *Inorg. Chem.* **2004**, *43*, 3406. doi:10.1021/IC049961V
[59] V. K. Ahluwalia, R. Aggarwal, *Comprehensive Practical Organic Chemistry: Preparations and Quantitative Analysis* **2005** (Universities Press (India) Pvt Limited: Hyderabad, Telangana).
[60] A. Kumbhar, S. Jadhav, R. Shejwal, G. Rashinkar, R. Salunkhe, *RSC Adv.* **2016**, *6*, 19612. doi:10.1039/C6RA01062H
[61] K. Kundu, S. K. Nayak, *RSC Adv.* **2012**, *2*, 480. doi:10.1039/C1RA00652E